Available online at www.sciencedirect.com

SCIENCE DIRECT

Vision Research 46 (2006) 2475–2486

Vision Research

www.elsevier.com/locate/visres

# The effect of binocular eye position and head rotation plane on the human torsional vestibuloocular reflex

Americo A. Migliaccio [a,*], Charles C. Della Santina [a], John P. Carey [a], Lloyd B. Minor [a], David S. Zee [b]

[a] *Department of Otolaryngology—Head and Neck Surgery, Johns Hopkins University, MA 21205, USA*
[b] *Department of Neurology, Johns Hopkins University, MA 21205, USA*

Received 20 July 2005; received in revised form 3 February 2006

**Abstract**

We examined how the gain of the torsional vestibulo-ocular reflex (VOR) (defined as the instantaneous eye velocity divided by inverted head velocity) in normal humans is affected by eye position, target distance, and the plane of head rotation. In six normal subjects we measured three-dimensional (3D) eye and head rotation axes using scleral search coils, and 6D head position using a magnetic angular and linear position measurement device, during low-amplitude (~20°), high-velocity (~200°/s), high-acceleration (~4000°/s$^2$) rapid head rotations or 'impulses.' Head impulses were imposed manually and delivered in five planes: yaw (horizontal canal plane), pitch, roll, left anterior-right posterior canal plane (LARP), and right anterior-left posterior canal plane (RALP). Subjects were instructed to fix on one of six targets at eye level. Targets were either straight-ahead, 20° left or 20° right from midline, at distance 15 or 124 cm from the subject. Two subjects also looked at more eccentric targets, 30° left or 30° right from midline. We found that the vertical and horizontal VOR gains increased with the proximity of the target to the subject. Previous studies suggest that the torsional VOR gain should decrease with target proximity. We found, however, that the torsional VOR gain did not change for all planes of head rotation and for both target distances. We also found a dynamic misalignment of the vertical positions of the eyes during the torsional VOR, which was greatest during near viewing with symmetric convergence. This dynamic vertical skew during the torsional VOR arises, in part, because when the eyes are converged, the optical axes are not parallel to the naso-occipital axes around which the eyes are rotating. In five of six subjects, the average skew ranged 0.9°–2.9° and was reduced to <0.4° by a 'torsional' quick-phase (around the naso-occipital axis) occurring <110 ms after the onset of the impulse. We propose that the torsional quick-phase mechanism during the torsional VOR could serve at least three functions: (1) resetting the retinal meridians closer to their usual orientation in the head, (2) correcting for the 'skew' deviation created by misalignment between the axes around which the eyes are rotating and the line of sight, and (3) taking the eyes back toward Listing's plane.


*Keywords:* Torsional vestibulo-ocular reflex; Vertical skew; Torsional quick-phase; Near viewing

## 1. Introduction

The vestibulo-ocular reflex (VOR) keeps images stable on the retina by rotating the eyes in the direction opposite to head motion. When a subject is viewing a far target during high-acceleration, head-on-body rotational 'impulses' (e.g., Aw et al., 1996), the gain of the horizontal or vertical VOR, defined as the instantaneous eye velocity divided by inverted head velocity, is ~1. During near-target viewing, the gain of the VOR for horizontal and vertical rotations is >1, increasing as the target becomes closer (e.g., Viirre, Tweed, Milner, & Vilis, 1986). This increase during near viewing compensates for the relative translation of the eyes with respect to the target during the head rotation, which becomes greater as the distance of the target decreases.

Unlike the horizontal and vertical components of the VOR, the gain of the torsional VOR when viewing a far

* Corresponding author. Fax: +1 410 614 7222.
*E-mail address:* amiglia1@jhmi.edu (A.A. Migliaccio).

0042-6989/$ - see front matter © 2006 Elsevier Ltd. All rights reserved.
doi:10.1016/j.visres.2006.02.008

target is only ~0.7 (e.g., Aw et al., 1996) during roll 'impulses' of the head, and the effect of viewing a near target is less clear. During passively induced, head-on-body, 'quasi sinusoidal' stimuli (1–2 Hz, peak velocity 100°/s) with far (7.2 m) and near (20 cm) targets, the gain of the torsional VOR decreases moderately with near viewing (from ~0.8 for far targets to 0.74) (Averbuch-Heller et al., 1997). During passive sinusoidal head rotation at 0.3 Hz and 30°/s peak velocity while subjects viewed straight-ahead targets at 1.40 or 0.25 m that moved with the head (a context that could call for cancellation of the VOR), the torsional VOR gain decreased with the closer target by ~35% (Bergamin & Straumann, 2001). In contrast, in a study in rhesus monkeys, there was no change in the gain of the torsional VOR (transient stimulus at 60°/s and 220°/s$^2$) with viewing straight-ahead targets at (15, 20, 30, and 40 cm) (Green & Angelaki, 2003).

Ocular counter-roll following pure roll head rotations occurs around an axis parallel to the naso-occipital axis. Thus, when the eyes are converged on a near target, a vertical misalignment of the eyes (a 'skew deviation') develops following head roll, because the optical axes are not parallel to the axes around which the head and eyes are rotating (Fig. 1A). A lower *static* ocular counter-roll gain after head roll with near viewing could lessen the amount of vertical skew, thereby simplifying central processing of images required to achieve stereopsis (Mandelli, Misslisch, & Hess, 2005; Misslisch, Tweed, & Hess, 2001; Ooi, Cornell, Curthoys, Burgess, & MacDougall, 2004).

It is less clear what the *dynamic* counter-roll response is during head rotation with a roll component. Different studies have reported different amounts of vertical skew during roll head rotations (Jáuregui-Renaud, Faldon, Clarke, Bronstein, & Gresty, 1996, 1998; 2001 (skew ~6–8°); Bergamin & Straumann, 2001 (skew ~2°); and Pansell, Schworm, & Ygge, 2003 (skew ~3°)). Vertical skew during roll head motion likely depends on: (1) the starting position of the eyes in the orbit (based upon viewing distance and eccentricity); (2) the position, orientation and magnitude of the axis of head rotation; and (3) the gains of the torsional angular VOR and the vertical translational VOR. Thus the different vertical skews reported by these studies probably arise because of differences in the stimuli e.g., differences in the position and magnitude of the axis of roll head rotation.

In view of the conflicting evidence about the effect of viewing distance on the torsional VOR gain during rotation of the head, we examined the dependence of the tor-

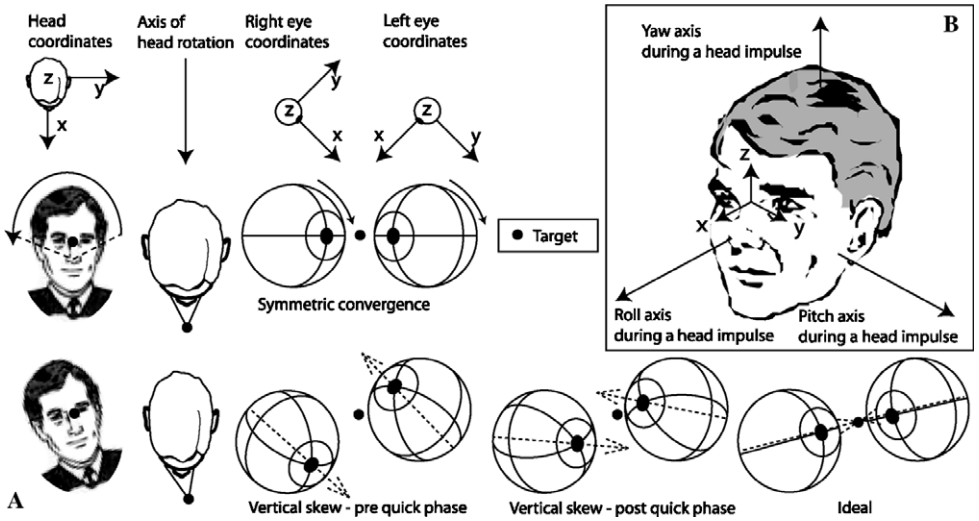


Fig. 1. (A) Qualitative cartoon showing vertical skew after a roll head rotation before and after a torsional quick-phase. The top traces show how the eye and head coordinate systems are misaligned during near viewing; thus, during near viewing a purely torsional eye rotation in head coordinates has torsional and vertical components in eye coordinates. The middle traces depict the positions of the left and right eyes just before roll rotation of the head when viewing a near target and both eyes are adducted equally. The bottom traces shows the final position of the eyes after a clockwise roll head impulse prior to a resetting torsional quick-phase. Note the eyes are in a space-fixed view and the angles are exaggerated. The expected response of the torsional VOR is to rotate both eyes around the naso-occipital axis in the counter-clockwise direction (the compensatory direction), which produces a difference in vertical eye position as reflected in the different locations to which the foveae are pointed. The amount of vertical disparity (skew) between the eyes depends on: (a) the gain of the torsional VOR—a larger torsional VOR gain will result in a larger eye rotation about an axis parallel to the naso-occipital axis and more vertical skew; (b) eye position—a more symmetrical adduction and/or larger adduction angle will result in more vertical skew; and (c) the axis of head rotation—during roll head impulses the otoliths are stimulated by vertical translations in opposite directions (hence moving the eyes in opposite vertical directions), so that the amount of otolith stimulation (and resulting vertical skew) depends on the position and magnitude of the axis of head rotation. The bottom traces also show the final position of the eyes post torsional quick phase in the clockwise (anti-compensatory) direction, which reduces vertical skew, bringing the eyes toward their final static counter-roll position and closer to the ideal fixation position for both eyes. (B) Head coordinate system, where $X$, $Y$, and $Z$ axes are perpendicular to the coronal, sagittal and transverse planes, respectively. The origin is located at the intersection of the mid-sagittal plane and the inter-ocular axis (the nasion). The axis of head rotation during a head impulse is often offset to the corresponding coordinate system axis. For example, during a roll head impulse the axis of head rotation is parallel to the $X$-roll axis, but offset 50 mm inferior to the head coordinate system origin.

sional VOR gain on target distance and eccentricity during high acceleration, brief duration, passive, head-on-body 'head impulse' rotations. To study vestibular mechanisms independent of immediate visual feedback and prediction, the timing and direction of the impulses were randomized, and the analysis was limited to the first ~100 ms of the responses, before any visual feedback might influence the response. We also measured vertical skew during the head rotation and we examined and quantified the corrective eye movements that reduced this skew.

## 2. Methods

### 2.1. Subjects

We studied six normal subjects (mean age 43; range 32–60 years). No subject had a history or clinical signs of vestibular disease. All had good stereo acuity and no history of ophthalmologic problems. Each subject was able to fuse vision without the aid of contact lenses or glasses at both 15 and 124 cm. The average inter-pupillary distance was 6.4 ± 0.2 cm. Participation in this study was voluntary, and the study was performed in accordance with a protocol approved by the Johns Hopkins School of Medicine Institutional Review Board.

### 2.2. Recording system

Angular eye and head positions were measured using dual search coils (manufactured by Skalar, Delft, The Netherlands) and a field coils system. The field-coil system consists of a cubic-coil frame (102 cm each side) producing three orthogonal magnetic fields (frequencies: 55.5, 83.3, and 41.6 kHz; intensity: 0.088 G). The dual search coils yield two sensitivity vectors, each characterized by voltages induced in one of the two coils by the three orthogonal fields. In vitro calibration is performed before each experiment in which voltage offsets are nullified by placing the coils into a metallic tube that completely shields the coil from the magnetic fields. The dual search coil then is placed on a gimbal system located in the center of the magnetic-coil frame. Coil gains are determined by aligning the sensitivity vectors of each coil with each of the three magnetic fields. Further details of the calibration and recording procedures can be found in Straumann, Zee, Solomon, Lasker, and Roberts (1995). Binocular eye movements were recorded in three-dimensions using dual search coils (two orthogonal coils embedded in a single silastic annulus) were placed on each eye. A dual search coil embedded in a bite block was used to measure head rotation. Eye and head angular positions were sampled at 500 Hz at 16-bit resolution. Analog (pre-sampled) signals were low-pass filtered with a single-pole analog filter that had a 3-dB bandwidth of 100 Hz. Digital (post-sampled) signals were filtered with a 50-tap zero-phase low pass digital finite impulse response filter with bandwidth 50 Hz.

Head movements were also recorded with a 6D miniBIRD device (Ascension Technology) that determines the 3D position and 3D orientation of a receiver with respect to a transmitter. During the sample interval the miniBIRD transmitter generates three orthogonal pulsed direct-current (DC) magnetic fields separate in time. The receiver is a hall probe, which measures the relative orientation of the receiver to each magnetic field. The maximum frequency content of the magnetic fields emitted by the device is 38 kHz, however, most of the spectral power is between DC and 13.5 kHz (a 30-dB drop in spectral power occurs across this range). The receiver was embedded in the bite block worn by the subject (as was the head rotation search coil), while the transmitter was fixed in space at a distance of ~35 cm from the subject. The resolution of the miniBIRD device was 0.5 mm RMS for position and 0.1°RMS for orientation, at 30 cm from the transmitter (manufacturer's specification). Static position accuracy was 1.8 mm RMS averaged over a range of ±75 cm in any direction. The analog signals from the miniBIRD device were sampled and processed simultaneously with the signals from the field coil system.

We tested signal interference between the coils system and the miniBIRD device. Linear translations of the mouthpiece (containing the dual search coil and miniBIRD receiver) in a $\pm 10\ cm^3$ range from the center of the coils frame resulted in mean angular errors in the coils orientation of <0.1° RMS and mean positional errors of the miniBIRD receiver of <2 mm RMS. The mean (and standard deviation) angular error did not change when the miniBIRD was turned off, so this error was probably due to non-linearities in the magnetic fields. Similarly, the mean positional error did not change when the coils system was turned off, however, its standard deviation decreased ~10%.

A wall-mounted laser positioned directly in front of the subject was rotated to project either an Earth-horizontal or Earth-vertical beam, which passed through the center of the magnetic field frame. Using this laser we positioned the subject (seated upright) so that the horizontal beam passed approximately over the center of both eyes (the eyes were closed) and the vertical beam passed over the midline (bisecting the nose). In the anterior–posterior direction the subject was positioned so that the anterior aspect of the lateral edge of the bony orbit was at the center of the fields. With this approach we could ensure that the subject's eyes and head coils remained in the linear region of the magnetic field for a large range of head movements.

The subject's head was positioned so that Frankfurt's line (from the superior most point of the bony-cartilaginous junction of the external auditory canal to the nadir of the cephalic edge of the infraorbital rim) was in the earth-horizontal plane. Once the subject's head was in the correct position the instantaneous 6D head position output from the miniBIRD device was recorded and used as the zero reference position. With the head at reference position, we measured the vertical and horizontal distance of the bite block (located in the mid-sagittal plane) from the inter-ocular axis (defined by the line passing through the center of both eyes). During each trial, the room was completely dark except for a light-emitting diode (LED) placed at one of six positions and some glow from the monitor display that faced the head impulse operator. The LED was at eye level and located either straight-ahead, 20° left or 20° right from midline, at distance 15 or 124 cm from the subject. Two subjects fixed on two additional LED positions, either 30° left or 30° right from midline. The head impulse operator using a real-time graphical display of 6D head position ensured the head was at reference position before the start of each head impulse. During the first five seconds of each data file, eye, and head position were calibrated by instructing the subject to fix on the straight-ahead far target. Head impulses were delivered manually in five planes: yaw (semi-circular canal plane), pitch, roll, left anterior-right posterior canal plane (LARP), and right anterior-left posterior canal plane (RALP). The head rotations were unpredictable in sign. For example, randomly left or right for yaw head impulses. These head rotations consisted of passive, manually imposed rotations with peak amplitude ~20°, peak velocity ~200°/s and peak acceleration $\sim 4000°/s^2$ (Halmagyi & Curthoys, 1988).

### 2.3. Data analysis

Once the head was positioned at the zero reference position we defined the transverse plane as the plane parallel to Earth-horizontal passing through the Frankfurt's lines. The coronal plane was defined as the plane perpendicular to the transverse plane passing through the center of both orbits. The sagittal plane was defined as the plane perpendicular to both the transverse and coronal planes and passing through the nasion. The naso-occipital ($+X$ pointing anterior), inter-aural ($+Y$ pointing left), and superior-inferior axes ($+Z$ pointing superior) were defined as the vectors normal to the respective, coronal, sagittal, and transverse planes with origin located at the intersection of these planes (Fig. 1B).

Eye and head angular positions were represented by rotation vectors with roll, pitch, and yaw coordinates (Haslwanter, 1995; Migliaccio & Todd, 1999). The orientation of each eye relative to the head was also quantified as rotation vectors. Head-in-space, eye-in-space, and eye-in-head velocity vectors were calculated from the corresponding rotation vectors (Hepp, 1990). Head velocity was calculated with reference to a head-fixed coordinate frame (naso-occipital, inter-aural, and superior-in-

ferior axes are parallel to the corresponding roll, pitch, and yaw axes, respectively), so that eye and head velocities were expressed with reference to exactly the same coordinate frame (Aw et al., 1996). Eye and head velocity were also recalculated relative to an eye-fixed coordinate frame so that torsion would be referenced to the optic axis. Head rotations were always described as yaw, pitch and roll. Eye rotations were described as horizontal, vertical and torsional. Eye and head rotations are always with respect to a head-coordinate system, unless an eye coordinate system is specified.

To calculate vertical ocular misalignment (skew), the positions of the eyes were represented using Helmholtz angles in head coordinates (Haslwanter, 1995). In head coordinates there will only be a difference in the vertical component of the 3D Helmholtz angle between the eyes when both eyes are not pointing at the same location in space. Hence, vertical skew was calculated as the difference in vertical Helmholtz position between the eyes.

The time of onset of each head impulse was identified by fitting a polynomial curve to head-in-space velocity versus time. The point where the magnitude of the fitted curve was greater than 2% of the curve's peak magnitude (typically this threshold was ~4°/s) was defined as the time of onset. A similar approach was used to identify the time of onset of the eye movement responses. As the time between the onset of the impulse and its maximum velocity was less than 150 ms, analysis of the impulse data was restricted to a period of 150 ms from the onset.

Start and end of a quick phase were defined as the points at which eye acceleration rose above or fell below manually estimated maximum slow phase eye acceleration, respectively. Quick-phase amplitude was defined as the difference in angular eye position between the start and end of the quick phase. Quick-phase peak velocity was defined as the difference in minimum and maximum eye velocity during the quick phase.

The eye movement response to head impulses delivered in the LARP and RALP planes has both vertical and torsional components of eye velocity. These components were analyzed separately both in eye and head coordinates, because we wanted know the actual rotation of the eye around the optic axis when eye position changed in the orbit. The vertical components of eye and head velocity were used to calculate the gain of the vertical VOR during RALP and LARP head impulses. Similarly, the torsional components of eye and head velocity were used to calculate the gain of the torsional VOR.

Trials of head impulse data that included blinks or in which the subject did not fix upon the near target with both eyes at the onset of head rotation, were not included in the analysis. Depending on the subject, approximately 10–20% of trials were rejected for this reason. The 3D VOR gains, for head impulses delivered in all planes, were calculated by dividing each component of inverted eye velocity by the corresponding component of head velocity during the 30 ms period prior to peak head velocity and averaged across trials. Counter-roll gain was calculated by dividing the negative of the torsional component of the rotation vector representing eye position by the torsional component of the rotation vector representing head position.

### 2.4. Statistical analysis

For pitch, roll, LARP, and RALP impulse data the gains of the VOR calculated separately for each eye were not significantly different (MANOVA, $P = 0.90$), so gains were pooled across the two eyes. Although there was a trend towards a difference between horizontal VOR gains calculated using the left eye vs. the right eye during near viewing, this difference was not statistically significant (MANOVA, $P = 0.08$), so these left and right eye data were pooled, as well. Since there was no significant difference between head impulses in opposite directions within the same plane (MANOVA, $P = 0.21$) the gains for each direction were pooled (e.g., during yaw head rotations the VOR gains during leftward and rightward rotations).

All results are described as means ± 1 SD. A multi-way analysis of variance was used to compare the data from more than two groups (Diggle, Liang, & Zeger, 1994). The variables included in the model were: subject identifier, coordinate system (eye or head coordinates), target distance (near or far), target position (left 30°, left 20° straight-ahead, right 20°, right 30°), rotation plane (yaw, pitch, roll, LARP, and RALP) and VOR gain component (horizontal, vertical, torsional, LARP, and RALP), axis of head rotation position ($X$, $Y$, and $Z$), orientation (unit velocity vector $X$, $Y$, and $Z$ components) and magnitude. Data from two groups were compared with unpaired $t$ tests. Paired $t$ tests were used when comparing data from the same subject.

### 2.5. Head rotation axis

Using the 3D orientation position data from the scleral coils, 3D translational position data from the miniBIRD device, and the anatomical distances (Frankfurt's plane; distance of miniBIRD receiver from inter-aural axis) we calculated the position, magnitude, and orientation of the axis of head rotation for each subject, impulse plane, and fixation condition (target position). The instantaneous position of the center of head rotation ($X_{COR}$, $Y_{COR}$, and $Z_{COR}$) in head coordinates was calculated by solving the formula below:

$$\begin{bmatrix} X_{final} - X_{COR} \\ Y_{final} - Y_{COR} \\ Z_{final} - Z_{COR} \end{bmatrix} = \begin{bmatrix} \cos(\theta_H)\cos(\varphi_H) & -\sin(\theta_H)\cos(\varphi_H)\cos(\psi_H) + \sin(\varphi_H)\sin(\psi_H) & \sin(\theta_H)\cos(\varphi_H)\sin(\psi_H) + \sin(\varphi_H)\cos(\psi_H) \\ \sin(\theta_H) & \cos(\theta_H)\cos(\psi_H) & -\cos(\theta_H)\sin(\psi_H) \\ -\cos(\theta_H)\sin(\varphi_H) & \sin(\theta_H)\sin(\varphi_H)\cos(\psi_H) + \cos(\varphi_H)\sin(\psi_H) & -\sin(\theta_H)\sin(\varphi_H)\sin(\psi_H) + \cos(\varphi_H)\cos(\psi_H) \end{bmatrix} * \begin{bmatrix} X_{initial} - X_{COR} \\ Y_{initial} - Y_{COR} \\ Z_{initial} - Z_{COR} \end{bmatrix}$$

where ($X_{initial}$, $Y_{initial}$, and $Z_{initial}$) and ($X_{final}$, $Y_{final}$, and $Z_{final}$) are the instantaneous positions of the miniBIRD receiver at time t1 (initial) and t1 + sample-interval (final) in head coordinates during the head rotation; and ($\theta_H$, $\varphi_H$, and $\psi_H$) are the horizontal, vertical and torsional Helmholtz angles describing the head (and miniBIRD receiver) rotation during the sample interval (t1 to t1 + sample-interval). We calculated and used for our analysis the mean center of rotation of the head (COR) at peak head velocity. This simplification was justified because the change in mean position of the COR was small (<3 mm) during the 15 ms period before and after peak head velocity i.e., when the change in angular position is greatest. The orientation and magnitude of the 3D head velocity vector ($X$-roll, $Y$-pitch, and $Z$-yaw component of 3D angular velocity) were calculated at peak head velocity, which was the point at which all components of the 3D velocity tended to deviate maximally from baseline. Table 1 shows the magnitude, orientation and point closest to the origin (calculated using the orientation of the axis of head rotation and the COR) through which the axis of head rotation must pass. The variation in axis orientation was calculated by determining the mean angle between the normalized 3D head velocity unit vectors representing individual trials and the mean 3D head velocity unit vector. Similarly, variation in COR was calculated by determining the mean distance between the 3D COR for individual trials and the mean 3D COR. These techniques are similar to previously published methods of comparing vectors (e.g., Della Santina, Potyagaylo, Migliaccio, Minor, & Carey, 2005).

For each subject the variation in the orientation and position of the axis of head rotation for each head rotation plane is small (<4° and <5 mm). The variation in the velocity magnitude of the axis of head rotation was <25°/s. In addition, for each subject, the magnitude, orientation and position of the axis of head rotation for each head rotation plane, did not change with target distance (MANOVA; $P > 0.05$ (magnitude, for all subjects), $P > 0.20$ ($X$, $Y$, $Z$ components of 3D head velocity

Table 1
Mean (±1SD) position, orientation and magnitude of the axis of head rotation for each rotation plane ($n = 4$)

| Rotation Plane | Position (mm) | | | Orientation (°) | | | Magnitude (°/s) |
|---|---|---|---|---|---|---|---|
| | $X$ | $Y$ | $Z$ | Coronal (±) $X$ | Sagittal (±) $Y$ | Transverse (±) $Z$ | |
| YAW | $-70.1 \pm 1.8$ | $-1.3 \pm 1.5$ | $0.5 \pm 1.6$ | $+0.7 \pm 1.6$ | $-0.1 \pm 1.9$ | $+89.7 \pm 1.3$ | $218 \pm 14$ |
| PITCH | $-47.6 \pm 3.5$ | $-0.1 \pm 3.3$ | $-102.9 \pm 3.3$ | $+0.5 \pm 1.8$ | $+87.6 \pm 2.6$ | $+2.3 \pm 2.9$ | $206 \pm 24$ |
| ROLL | $-0.6 \pm 1.7$ | $1.8 \pm 2.6$ | $-50.3 \pm 1.9$ | $+88.5 \pm 3.1$ | $-0.3 \pm 2.8$ | $+1.6 \pm 2.7$ | $195 \pm 17$ |
| LARP | $17.4 \pm 3.8$ | $18.3 \pm 4.1$ | $-100.3 \pm 2.5$ | $-43.4 \pm 3.6$ | $+46.5 \pm 3.3$ | $-2.2 \pm 3.0$ | $193 \pm 19$ |
| RALP | $18.2 \pm 2.8$ | $-17.1 \pm 3.9$ | $-100.6 \pm 3.1$ | $+43.8 \pm 3.2$ | $+46.2 \pm 3.5$ | $-1.4 \pm 2.9$ | $192 \pm 18$ |

Position ($X$, $Y$, and $Z$ in mm) gives the location of the point closest to the origin of the head coordinate system through which the axis of head rotation passes. For example, during a roll head rotation the axis of head rotation passes through a point approximately on the sagittal plane and 50 mm below the transverse plane (or ~50 mm below the nasion). Orientation denotes the angle (0–90°) that the unit velocity vector subtends with the coronal, sagittal and transverse planes. The sign (±) of the $X$, $Y$, and $Z$ components of the unit velocity vector (positive for leftward, downward, clockwise, downward and counter-clockwise (LA), downward and clockwise (RA) head rotations) are included to resolve in which (two) of the (eight) sectors (created by the intersection of three planes) the axis of head rotation lies.

unit vector, for all subjects), $P > 0.10$ ($X$, $Y$, and $Z$ components of position, for all subjects)). For four of six subjects there was no difference in the magnitude, orientation and position in the axis of head rotation for each head rotation plane (MANOVA; $P > 0.05$, $P > 0.15$, and $P > 0.05$). If the remaining two subjects are included, then there is a small difference in the position (MANOVA; $P < 0.05$), and magnitude (MANOVA; $P < 0.05$), but not the orientation (MANOVA; $P > 0.10$), of the axis of head rotation.

### 2.6. Listing's plane

Listing's Law states that when the head is upright and not moving, the three-dimensional positions (horizontal, vertical, and torsional) that the eye can adopt are constrained such that when they are expressed as a single-axis rotation from a fixed reference position, the resulting axes all lie in a single head-fixed plane known as the 'displacement' plane (Haustein, 1989; Helmholtz, 1867). The orientation of the displacement plane changes when the reference eye position is changed. The reference eye position can be represented by a reference gaze vector, which is a vector parallel to the line-of-sight when the eye is at the reference position. When the reference gaze vector is perpendicular to the resulting displacement plane, it represents a unique reference eye position called 'primary position (LPP),' and the associated unique displacement plane is 'Listing's plane (LP).' Listing's law is obeyed during steady fixation and also during saccadic and smooth-pursuit eye movements i.e., the (single-axis) rotation vectors representing instantaneous eye position during these eye movements all lie in a single plane (e.g., Tweed & Vilis, 1990).

With the head fixed at the zero reference position LP and LPP for each subject was calculated from the eye position rotation vectors (using the method described by Tweed, 1997) measured as the subject repeatedly fixed upon nine targets positioned at 0°, ±20° horizontal and ±20° vertical eccentricity, directly in front of the subject, at 15 cm and then at 124 cm for a 60-s period. A best fit for Listing's Plane was determined using a singular value decomposition algorithm (Press, Flannery, Teukolsky, & Vetterling, 1988):

$$r_x = f + f_v r_y + f_h r_z$$

in which $r_x$, $r_y$, and $r_z$ are the components of the rotation vector representing the torsional, vertical and horizontal components of the rotation in head coordinates and $f$, $f_v$, and $f_h$ are coefficients.

## 3. Results

### 3.1. VOR gain

The mean horizontal and vertical VOR gains (during pure horizontal and vertical head impulses) across all far viewing conditions and across all subjects were $0.95 \pm 0.06$ and $1.04 \pm 0.03$, respectively (Fig. 2). None of the subjects ($n = 6$) generated a quick-phase earlier than 150 ms after the onset of the head impulse. The horizontal and vertical VOR gains (in a head-coordinate system) were ~35% greater during near (15 cm) than far (124 cm) target viewing ($P < 0.05$ for all subjects) (Fig. 2). The gains of the horizontal or vertical VOR did not change significantly with target eccentricity (MANOVA: horizontal VOR $P = 0.39$, vertical VOR $P = 0.75$).

The mean individual torsional VOR gains (during pure roll head impulses while viewing a near target straight-ahead) ranged from $0.43 \pm 0.04$ to $0.80 \pm 0.05$. Individual gains for each person did not change with target distance (MANOVA: $P = 0.53$), target eccentricity (MANOVA: $P = 0.68$), or plane of head rotation (MANOVA: $P = 0.72$).

The center of head rotation (and consequent pattern of otolith stimulation) was different during pure pitch, pure roll, RALP and LARP stimuli. For the RALP, and LARP stimuli, the centers of rotation were about 2 cm in front of the eyes, about 10 cm below the inter-ocular axis, and about 2 cm from the mid-sagittal plane, making it farther from the otoliths than was the case for the pure pitch and pure roll stimuli (Table 1). Even so, the VOR responses to pure pitch and pure roll stimuli were the same as the vertical and the torsional components of the response to LARP and RALP stimuli when pooled for all viewing conditions (vertical VOR vs. vertical component of LARP and RALP VOR coefficients = 0.98, $P < 0.05$, $R^2 = 0.76$; torsional VOR vs. torsional component of LARP and RALP VOR coefficients = 0.94, $P < 0.05$, $R^2 = 0.62$). Thus, for these head impulses, the direction and magnitude of otolith stimulation (~0.3 g during roll and pitch, and ~0.7 g during RALP and LARP) did not affect the gain of the torsional VOR.

We analyzed the vertical, torsional, RALP, and LARP VOR further comparing the eye movement responses in head and in eye coordinates. In *head* coordinates, the vertical component of the 3D VOR gain was 25–35% greater during near viewing than during far viewing ($P < 0.05$),

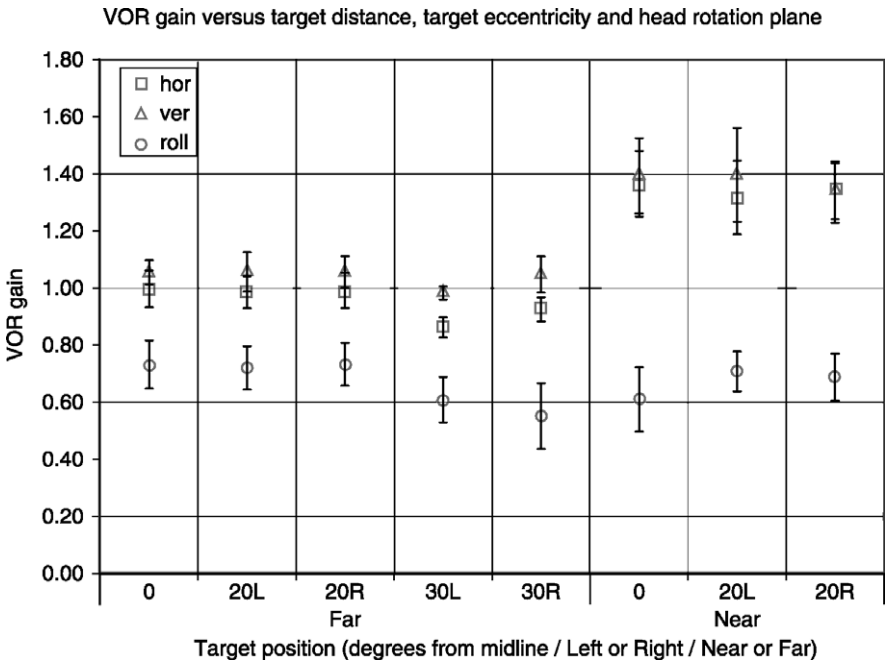


Fig. 2. Horizontal, vertical, and torsional VOR gains (in a head coordinate system) for all eight viewing conditions. The gains were calculated from the head rotations in the corresponding plane (yaw, pitch, and roll). The horizontal and vertical VOR gains change with target distance, but not with eye eccentricity. In contrast, the torsional VOR gain did not change significantly with target distance or eye eccentricity. Error bars denote ± 1SD.

and at far viewing did not depend significantly on target eccentricity up to ±30°. During near viewing, the vertical component of the 3D VOR gain decreased with increasing eccentricity ($P < 0.05$) when computed in *head* coordinates. In *eye* coordinates, however, the vertical component of the VOR gain (during LARP head rotation and leftward target viewing, or during RALP head rotation and rightward target viewing) was ~35% greater during near viewing and did not change with target eccentricity ($P = 0.72$).

In *head* coordinates, the torsional component of the 3D VOR gain did not change with viewing distance, eccentricity, or plane of rotation. In *eye* coordinates, however, with torsion around the line of sight, the torsional component of the VOR gain (during LARP head rotation and rightward target viewing, or during RALP head rotation and leftward target viewing) during near viewing increased with target eccentricity, by ~10% when fixating a near target 20° off midline ($P < 0.05$). The difference in the torsional and vertical VOR gains between eye and head coordinate systems is illustrated in Fig. 3 (data from subject five), and shows the importance of using an *eye* coordinate system to define the actual motion of images on the retina.

For all subjects, during pure roll head rotations with far viewing, the latencies were 103.1 ± 16.2 ms (range, 84–127 ms) after the onset of the impulse with the velocity and amplitude ranging between 75 and 180°/s and 0.6–5.4°, respectively (Table 2).

A representative response from the same subject whose data are shown in Fig. 3 is shown in Fig. 4 (subject five). During a roll head impulse (while viewing a straight-ahead

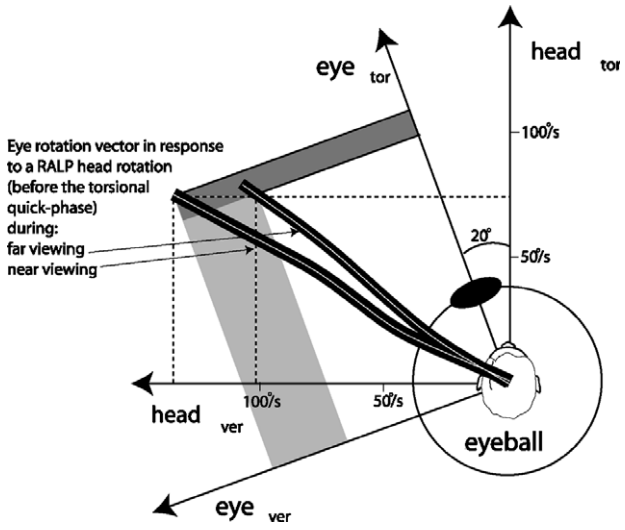


Fig. 3. The mean (± 1SD) vertical and torsional components of the eye velocity vectors at each sample time (starting from impulse onset to quick-phase onset) are plotted to show the axes of eye rotations in response to a RALP head rotation while viewing a far or near target (both 20°left from midline) in subject five. The horizontal dashed line denotes the point at which a torsional quick-phase occurs during near viewing and where RALP head velocity during far and near viewing is 142°/s. Note that peak torsional eye velocity is greater during far viewing because the quick-phase occurs later. The extra vertical component during near viewing (in head coordinates) changes the projection of the eye rotation axis onto the torsion axis in eye coordinates (optic axis: torsion). The region in dark gray shows the extra torsional component in eye coordinates. The torsional component in head coordinates, however, remains the same for both viewing conditions. The region in light gray shows the extra vertical component in eye coordinates. The change in vertical component with near viewing is larger in head than in eye coordinates.

Table 2
Torsional quick-phase parameters during pure roll head impulses

| ID | Torsional quick-phase parameters | | | | | | | | VOR |
|---|---|---|---|---|---|---|---|---|---|
| | Far target at 0° | | | | Near target at 0° | | | | Near target at 0° |
| | Latency (ms) | Velocity (°/s) | Amplitude (°) | Duration (ms) | Latency (ms) | Velocity (°/s) | Amplitude (°) | Duration (ms) | Slow phase gain |
| 1 | 100 ± 8 | 75 ± 14 | 2.0 ± 0.7 | 63 ± 13 | 74 ± 10 | 94 ± 19 | 2.4 ± 1.0 | 75 ± 12 | 0.43 ± 0.05 |
| 2 | 109 ± 9 | 143 ± 22 | 3.1 ± 1.0 | 74 ± 14 | 86 ± 13 | 175 ± 24 | 3.4 ± 0.9 | 78 ± 10 | 0.52 ± 0.07 |
| 3 | No QP. | No QP. | No QP. | No QP. | No QP. | No QP. | No QP. | No QP. | 0.56 ± 0.03 |
| 4 | 127 ± 8 | 89 ± 14 | 0.6 ± 0.9 | 23 ± 11 | 100 ± 12 | 105 ± 16 | 1.0 ± 0.9 | 33 ± 12 | 0.60 ± 0.09 |
| 5 | 84 ± 7 | 180 ± 21 | 5.4 ± 1.1 | 86 ± 23 | 69 ± 10 | 260 ± 32 | 7.6 ± 1.5 | 91 ± 9 | 0.74 ± 0.11 |
| 6 | 96 ± 11 | 166 ± 26 | 3.2 ± 1.3 | 67 ± 19 | 90 ± 11 | 195 ± 27 | 3.6 ± 1.2 | 84 ± 13 | 0.80 ± 0.13 |

The target is located straight ahead for both near (15 cm) and far viewing (124 cm) conditions. The amplitude and peak velocity of the quick phases (QP) tended to be greater in subjects with higher torsional VOR gains.

far target) (Fig. 4A), before any quick phases, the (inverted) torsional eye velocity trace was similar in shape to the head velocity trace, although slightly smaller in magnitude. At 84 ms after the onset of the stimulus, an anti-compensatory torsional quick phase occurred. During near viewing (Fig. 4B), this subject generated a torsional quick phase at an even earlier latency (69 ms). The same five subjects who generated torsional quick phases with far viewing also did so for near viewing. The quick phases during near viewing occurred on average 83.8 ± 12.8 ms (range, 69–100 ms, $n = 5$) after the onset of the impulse. Whereas, the quick-phases during far viewing occurred on average 19.3 ± 8.1 ms later ($P < 0.05$, mean paired difference between near and far for the five subjects). The torsional quick phases with near viewing had larger amplitudes (mean: 3.6 ± 2.5°, $n = 5$; $P < 0.06$), durations (mean: 72 ± 23 ms, $n = 5$; $P < 0.05$) and peak velocities (mean: 166 ± 68°/s, $n = 5$; $P < 0.05$) when compared with quick-phases that occurred during far viewing (amplitude mean: 2.9 ± 1.8°; duration mean: 63 ± 24 ms; peak velocity mean: 131 ± 47°/s, $n = 5$) (Table 2).

### 3.2. Vertical skew and corrective quick phases

Fig. 5 shows representative eye and head *positions* during a clockwise roll impulse in the same subject whose data are shown in Fig. 4 (subject five). In this subject the maximum vertical skew while viewing a straight-ahead far target was <0.2° (for all subjects <0.4°, mean 0.25 ± 0.14°, $n = 6$), whereas while viewing a straight-ahead near target, the maximum vertical skew before the quick phase was 1.4 ± 0.9°. The mean (across subjects) maximum vertical skew during a roll head impulse while viewing a straight-ahead near target (before the quick-phase) was 1.6 ± 0.7° (range 0.9–2.9°, $n = 6$). This vertical skew during near viewing, however, decreased with target eccentricity; for targets 20° left and 20° right from midline the mean maximum vertical skew was 0.9 ± 0.4° (range 0.5–1.9°, $n = 6$). In the five subjects who made anti-compensatory quick phases before the head movement ended, skew was minimized to <0.4° (mean 0.26 ± 0.11°, $n = 5$). The amplitude, duration and peak velocity of the quick phase tended to be greater in subjects with higher torsional VOR gains, although this relationship was not statistically significant.

### 3.3. Counter-roll gain before and after the torsional quick phase

Instantaneous counter-roll gains (|eye position/head position|) *during* a roll head impulse were calculated at the beginning and the end of the torsional quick phase during both far and near viewing (Fig. 5). The counter-roll gain before the torsional quick-phase was similar during near and far viewing (far viewing mean gain 0.65 ± 0.11 vs. near viewing mean gain 0.57 ± 0.06, paired difference 0.08 ± 0.13, $n = 6$; $P = 0.20$). The counter-roll gain after the torsional quick phase, however, was significantly lower during near viewing (far viewing mean gain 0.45 ± 0.16 vs. near viewing mean gain 0.26 ± 0.10, paired difference 0.19 ± 0.11, $n = 5$; $P < 0.05$). There was no statistically significant relationship between reduction in counter-roll gain during the quick phase and the amplitude of the quick-phase.

### 3.4. Listing's law

While fixing upon an array of far targets (124 cm) the mean (across subjects) orientation of LP (described by LPP in head coordinates) for the left eye was −2.1 ± 1.2° vertical and 2.2 ± 1.5° horizontal. While fixing upon near targets (15 cm) LPP was (−2.6 ± 2.2°, 10.3 ± 2.6°). Similarly, while fixing upon far targets the mean right eye LPP was (−3.1 ± 1.6°, −2.6 ± 1.4°), whereas while fixing upon near targets LPP was (−1.2 ± 2.3°, −11.2 ± 2.8°). Thus, as the vergence angle increased from 1.5 ± 0.3° (when viewing the far target at 124 cm) to 23.7± 2.0° (when viewing the near target at 15 cm), on average LPP rotated leftward in the left eye by 8.1 ± 2.1° and rightward in the right eye by 8.6 ± 1.4°. The mean standard deviation of the thickness of Listing's plane for each eye across all subjects was 0.7 ± 0.3° during far viewing (range: 0.4–1.1°) and 1.0 ± 0.4° during near viewing (range: 0.6–1.5°).

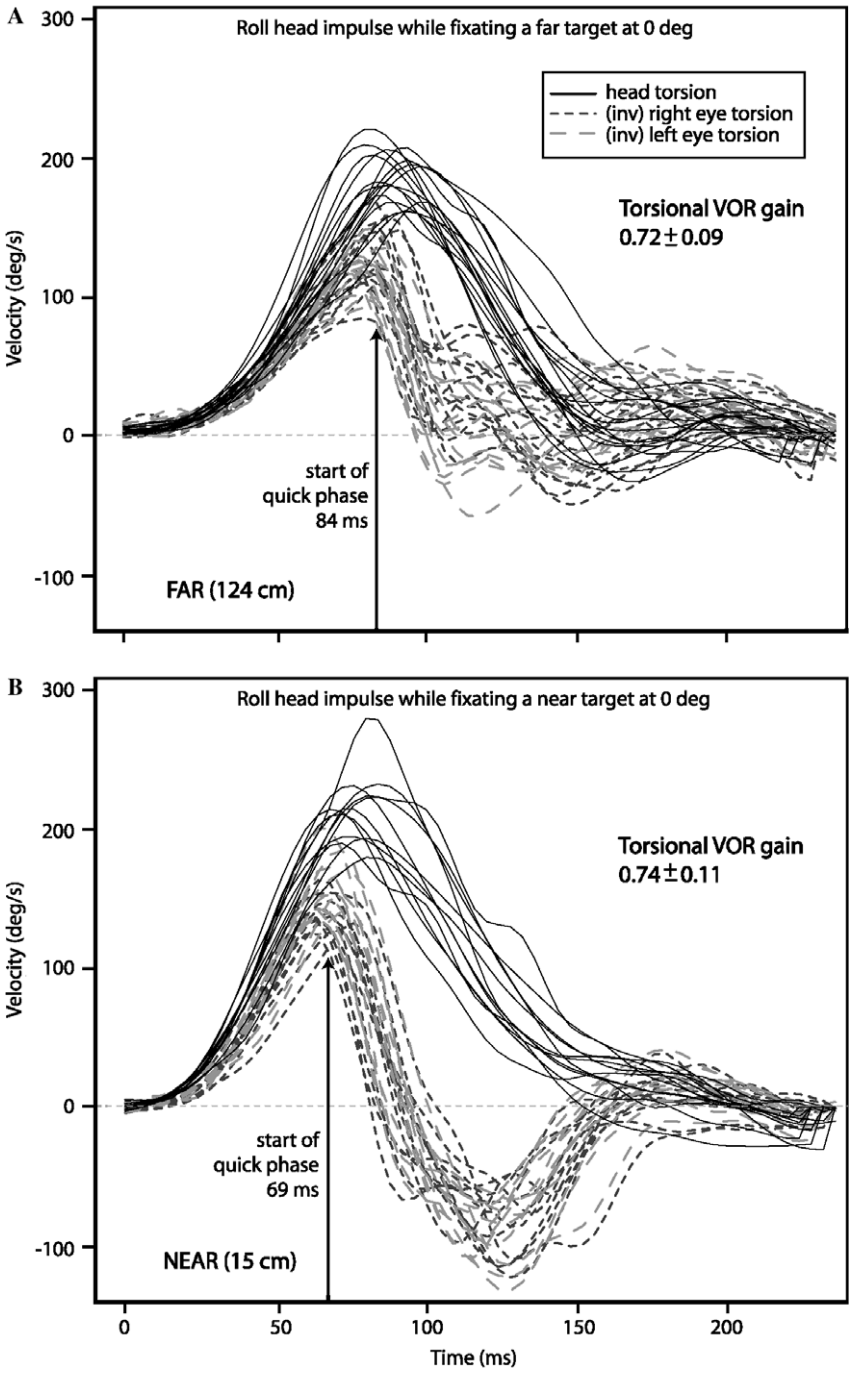


Fig. 4. Torsional quick phases during a clockwise head impulse in subject five. The target is located straight ahead for both near (15 cm) and far viewing (124 cm) conditions. The torsional VOR gain is the same during both far and near viewing. A torsional quick phase is generated during both viewing conditions; however, the anti-compensatory torsional quick phase occurs earlier and has a greater peak velocity during near viewing compared to far viewing.

During near viewing (target on midline and at eye level) and roll head impulses, the position of the eye at the start of the torsional quick phase (when head position was about $\pm 10^\circ$ roll) deviated in torsion, on average ($n = 5$), $\pm 7.6 \pm 3.4^\circ$ from Listing's plane (measured during near-viewing), whereas eye position at the end of the torsional quick-phase (when head position was $\pm 13^\circ$ roll) deviated only $\pm 3.1 \pm 2.1^\circ$ from Listing's plane (measured during near-viewing).

## 4. Discussion

### *4.1. The torsional VOR gain: Effect of near and far viewing and the plane of rotation*

The torsional component of the 3D VOR gain, i.e., the component of eye rotation about an axis parallel to the naso-occipital axis, was independent of viewing distance. This result was consistent across all subjects, but differs

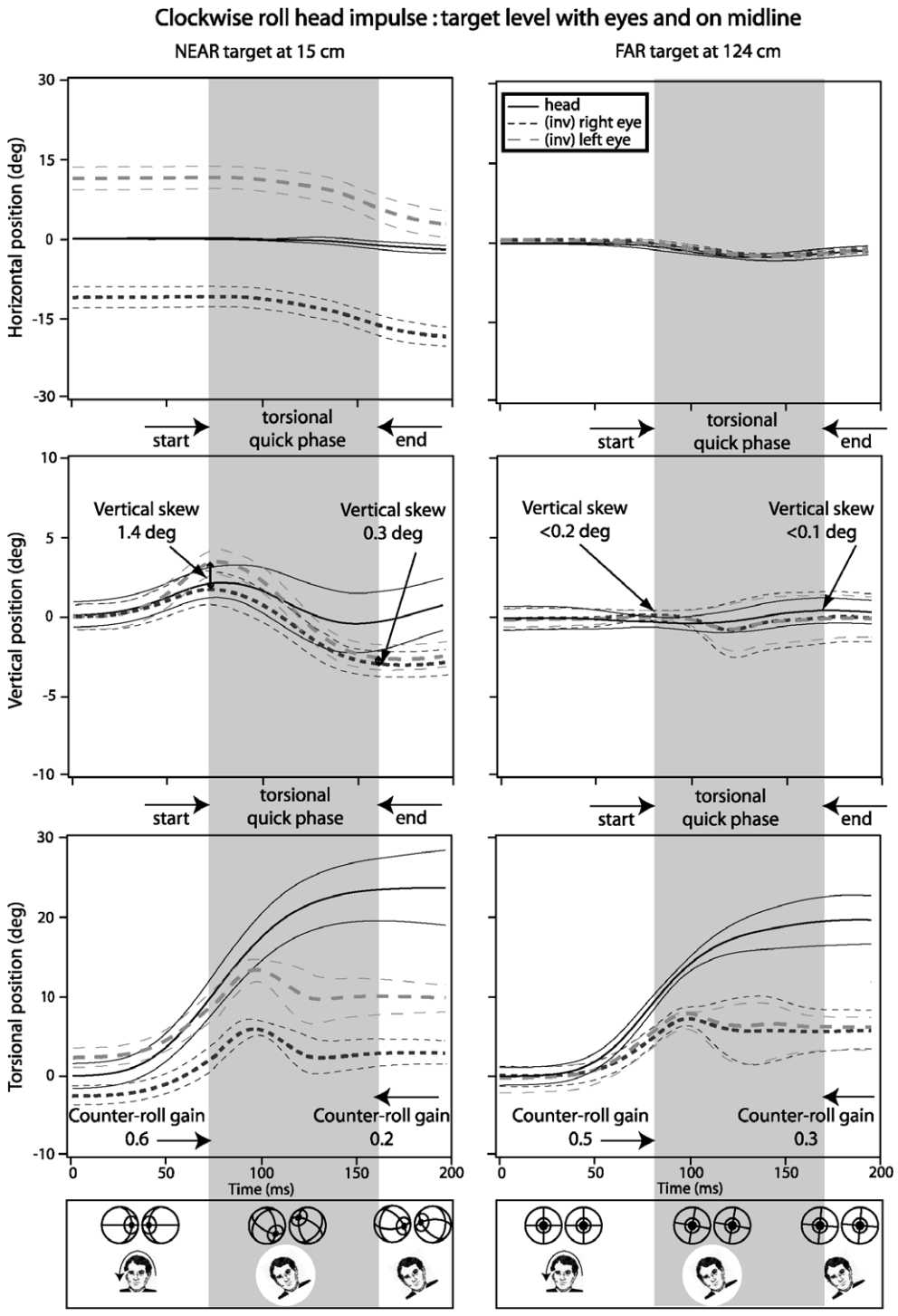


Fig. 5. The mean (±1 SD) of 3D angular eye and head position for subject five are shown during clockwise roll head impulses while viewing either a near or far target positioned on midline at eye level. The predominantly torsional eye rotation during the roll head impulse produced a vertical misalignment, or skew, between the eyes, which was reduced by an anti-compensatory torsional quick phase. The anti-compensatory torsional quick phase amplitude (gray region denotes the mean quick-phase duration) was larger during near viewing, resulting in a post-quick phase counter-roll gain that was smaller during near viewing. The change in horizontal eye position during near viewing was mostly due to the translational VOR response—as the head rolled, both eyes translated horizontally in the same direction, because the actual roll axis about which the head moved was ~5 cm inferior to the eyes. Torsional eye movements, which were around an axis parallel to the naso-occipital axis, also affected vertical eye position in eye coordinates (as shown by the vertical component of the Helmholtz angle plotted here) because the eyes were converged.

from some earlier reports that have described a decrease in torsional VOR gain for near-target viewing during sinusoidal head rotations (Averbuch-Heller et al., 1997; Bergamin & Straumann, 2001). Likewise, we also found no differences between the torsional VOR gain during roll, LARP and RALP stimulation, though Tweed et al. (1994) found a

higher torsional VOR gain when the stimulus also contained a pitch component. The discrepancies may be due to differences in stimuli. Previous studies have not examined the effect of near viewing on the torsional response to transient stimuli (head 'impulses' of high acceleration). The transient stimuli in this study went to higher peak velocities and had energy at frequencies higher than those in previous studies using sinusoidal stimuli. In addition, we restricted our analysis to the first ~100 ms of the response to non-predictable head impulses, before visual feedback or anticipation could influence the response.

### 4.2. What causes vertical skew during roll axis rotation of the head and near viewing?

During far viewing, a pure roll head rotation results in a pure torsional eye movement when measured both in eye and head coordinates. This is because the axis of head rotation is aligned with the optic axes and so the rotation is the same for both coordinate systems. During near viewing, however, the optic axes are not aligned with each other (because the eyes are offset laterally in the head) and therefore the axis of head rotation (which for a roll head rotation is parallel to the naso-occipital axis) can never align with both optic axes. Consequently, a purely torsional eye rotation in head coordinates, results in an eye rotation with torsional and vertical components in eye coordinates (Fig. 1A). When both eyes are adducting these vertical components are opposite in direction and thus produce a vertical ocular skew. For example, during a clockwise roll of the head while a subject views a near target, the angular VOR produces a counter-clockwise rotation of the eyes in head coordinates. In eye coordinates, however, the left eye rotates up and the right eye down (Fig. 1A). With the same stimulus the right otolith translates down and the left otolith translates up (a peak stimulus of ~0.3 g in our paradigm). Thus, if the translational VOR is also playing a role during a roll head rotation the right eye would rotate up and the left down (in head coordinates). These two effects—translation of the otoliths in opposite directions and misalignment of the optical and eye rotation axes—are in the opposite direction, so that any difference between their magnitudes would result in a residual skew deviation (Seidman, Leigh, Tomsak, Grant, & Dell'Osso, 1995a, 1995b).

### 4.3. How is vertical skew minimized?

How can vertical misalignment be minimized to prevent diplopia and ensure optimal binocular visual function? One possibility is to lower the torsional gain of the VOR during near viewing by an amount that varied with eye position, being greatest for symmetric convergence. Our data suggest this does not occur in response to passive head impulses, since the torsional VOR gain was independent of target distance and eye position. A second possibility is that stimulation of the otoliths would produce a disconjugate vertical eye movement (via the translational VOR) that would cancel the skew. However, this would require rapid processing of information from the otoliths and from the semicircular canals, as well as a signal encoding current eye position, to compute and produce the correct compensatory rotation of each eye in opposite directions. There is no evidence that the torsional angular VOR or the disconjugate vertical translational VOR could be adjusted quickly enough to prevent ocular skewing. Studies during eccentric rotations in which angular and linear acceleration are combined (Crane, Viirre, & Demer, 1997; Snyder & King, 1992) have suggested that the necessary adjustments in VOR gain for orbital translation, otolith stimulation and eye position take place over 40–100 ms, much later than would be required to account for the responses we observed. A third possible solution to this problem is to use the quick-phase mechanism to realign the eyes rapidly. Several groups have suggested a role for torsional quick phases in correcting the skew deviation (Jauregui-Renaud, Faldon, Gresty, & Bronstein, 2001; Misslisch & Hess, 2002). Also, otolith inputs have been noted to influence the pattern and dynamics of torsional quick phases (Groen, Bos, & de, 1999; Kori, Schmid-Priscoveanu, & Straumann, 2002). In our study, during near viewing, five of six subjects generated a torsional quick phase within the first 110 ms after the onset of the impulse. Quick phases were in the anti-compensatory direction and in these subjects reduced vertical skew on average from 1.6° to 0.3°. Although the torsional gain did not differ between near and far viewing, the size of the torsional quick phase was larger during near viewing, suggesting they might also play an important role in correcting the skew associated with near viewing.

### 4.4. How and why are torsional quick phases generated?

The fact that these rapid torsional eye movements occurred so early in response to the passive, unanticipated head rotation suggests that they are quick-phases generated by the vestibular system. In support of this idea there are other examples in which the saccade system generates early corrective rapid eye movements during passive head rotation. Labyrinthine defective patients, during high-frequency, high-velocity head rotations generate catch-up saccades at short latency, ~70 ms after stimulus onset (Della Santina, Cremer, Carey, & Minor, 2002; Halmagyi, Black, Thurtell, & Curthoys, 2003; Peng, Zee, & Minor, 2004, 2005; Tian, Crane, & Demer, 2000). These saccades are probably triggered by the vestibular system; they occur much earlier than visually-guided saccades, which typically have latencies of 90–130 ms (Becker, 1989). Although these 'vestibular catch-up saccades' typically occur during head rotations toward the side of an ear with vestibular hypofunction, the existence of these saccades suggests a neural substrate that allows saccades to be triggered by vestibular signals in normal subjects. Indeed, such early catch-up saccades are part of the response of normal subjects to pure translations of the head, augmenting the

response generated by the inherently under-compensatory slow-phase response (e.g., Ramat, Straumann, & Zee, 2005; Ramat & Zee, 2003; Tian, Crane, & Demer, 2003).

An alternative explanation is that a torsional quick phase is generated because the torsional position of the eye reaches the edge of the torsional oculomotor range during a roll head impulse. This would explain why the quick-phase amplitude tended to be greater in subjects with high torsional VOR gains, i.e., because the eyes counter-roll more in these subjects and a larger resetting quick phase would be required. The observation that torsional quick phases occur early in the response may be due to the fact that the torsional oculomotor range ($\sim \pm 25°$) is less than either the horizontal ($\sim \pm 50°$) or vertical ($\sim \pm 35°$) oculomotor range (Balliet & Nakayama, 1978; Guitton & Volle, 1987). This hypothesis, however, does not explain why the torsional quick phases had a lesser latency and larger amplitude during near viewing compared to far viewing, since there was no difference in torsional VOR gain during these two viewing conditions. Furthermore, the torsional quick phases occurred well before the eyes had rotated very far ($\sim 5°$), making it unlikely that a limit to torsion imposed by orbital constraints had been reached. Rather, we suggest that central mechanisms adjust the amplitude and latency of torsional quick phases based upon the target distance.

In addition to correcting for skew, torsional quick phases also can act to bring the eyes back to Listing's plane. At the same time, the torsional quick phases would realign the retinal meridians toward their usual position in the head during fixation (Groen et al., 1999; Jauregui-Renaud et al., 2001; Lee, Zee, & Straumann, 2000). This would, in effect, reduce the static counter-roll gain at the end of the head rotation and this effect would be greater at near viewing since the torsional quick phases are larger. Thus, the automatic occurrence of torsional quick phases early on during the head rotation helps to solve multiple potential problems created by torsional eye rotations in response to roll motion of the head during near viewing.

In summary, we have shown that during passive head impulses, the gain of the torsional VOR (as measured in head coordinates) is not influenced by viewing distance, plane of rotation or eye eccentricity. Torsional quick phases occur during roll rotations of the head. They are larger in amplitude and occur earlier for near viewing, and so reduce vertical skewing of the eyes, reorient the eyes back towards the horizontal meridian and bring the eye positions back towards Listing's plane.

## Acknowledgments

Supported by NIDCD grants (RO3 DC007346-01 to A.A.M., K08DC06216 to C.C.DS, K23 DC00196 and R03 DC005700 to J.P.C., R01 DC005040 to L.B.M. and RO1 EY001849 to D.S.Z.).

## References

Averbuch-Heller, L., Rottach, K. G., Zivotofsky, A. Z., Suarez, J. I., Pettee, A. D., Remler, B. F., et al. (1997). Torsional eye movements in patients with skew deviation and spasmodic torticollis: Responses to static and dynamic head roll. *Neurology, 48*, 506–514.

Aw, S. T., Haslwanter, T., Halmagyi, G. M., Curthoys, I. S., Yavor, R. A., & Todd, M. J. (1996). Three-dimensional vector analysis of the human vestibuloocular reflex in response to high-acceleration head rotations. I. Responses in normal subjects. *Journal of Neurophysiology, 76*, 4009–4020.

Balliet, R., & Nakayama, K. (1978). Training of voluntary torsion. *Investigative Ophthalmology and Visual Science, 17*, 303–314.

Becker, W. (1989). Metrics. In R. H. Wurtz & M. E. Goldberg (Eds.), *The neurobiology of saccadic eye movements* (pp. 13–67). Amsterdam: Elsevier.

Bergamin, O., & Straumann, D. (2001). Three-dimensional binocular kinematics of torsional vestibular nystagmus during convergence on head-fixed targets in humans. *Journal of Neurophysiology, 86*, 113–122.

Crane, B. T., Viirre, E. S., & Demer, J. L. (1997). The human horizontal vestibulo-ocular reflex during combined linear and angular acceleration. *Experimental Brain Research, 114*, 304–320.

Della Santina, C. C., Cremer, P. D., Carey, J. P., & Minor, L. B. (2002). Comparison of head thrust test with head autorotation test reveals that the vestibulo-ocular reflex is enhanced during voluntary head movements. *Archives of Otolaryngology–Head and Neck Surgery, 128*, 1044–1054.

Della Santina, C. C., Potyagaylo, V., Migliaccio, A. A., Minor, L. B., & Carey, J. P. (2005). Orientation of human semicircular canals measured by three-dimensional multiplanar CT reconstruction. *Journal of the Association for Research in Otolaryngology, 6*, 191–206.

Diggle, P. J., Liang, K. Y., & Zeger, S. L. (1994). *Analysis of longitudinal data*. New York: Oxford University Press.

Green, A. M., & Angelaki, D. E. (2003). Resolution of sensory ambiguities for gaze stabilization requires a second neural integrator. *Journal of Neuroscience, 23*, 9265–9275.

Groen, E., Bos, J. E., & de, G. B. (1999). Contribution of the otoliths to the human torsional vestibulo-ocular reflex. *Journal of Vestibular Research, 9*, 27–36.

Guitton, D., & Volle, M. (1987). Gaze control in humans: Eye-head coordination during orienting movements to targets within and beyond the oculomotor range. *Journal of Neurophysiology, 58*, 427–459.

Halmagyi, G. M., & Curthoys, I. S. (1988). A clinical sign of canal paresis. *Archives of Neurology, 45*, 737–739.

Halmagyi, G. M., Black, R. A., Thurtell, M. J., & Curthoys, I. S. (2003). The human horizontal vestibulo-ocular reflex in response to active and passive head impulses after unilateral vestibular deafferentation. *Annals of the New York Academy of Sciences, 1004*, 325–336.

Haslwanter, T. (1995). Mathematics of three-dimensional eye rotations. *Vision Research, 35*, 1727–1739.

Haustein, W. (1989). Considerations on Listing's law and the primary position by means of a matrix description of eye position control. *Biological Cybernetics, 60*, 411–420.

Helmholtz, H. V. (1867). Handbuch der Physiologischen Optik. Voss, Hamburg the oculomotor system in three dimensions. *Journal of Neurophysiology, 58*, 832–849.

Hepp, K. (1990). On Listing's Law. *Communications on Mathematical Physics, 132*, 285–295.

Jáuregui-Renaud, K., Faldon, M., Clarke, A., Bronstein, A. M., & Gresty, M. A. (1996). Skew deviation of the eyes in normal human subjects induced by semicircular canal stimulation. *Neuroscience Letters, 235*, 135–137.

Jáuregui-Renaud, K., Faldon, M., Clarke, A. H., Bronstein, A. M., & Gresty, M. A. (1998). Otolith and semicircular canal contributions to the human binocular response to roll oscillation. *Acta Otolaryngology (Stockholm), 118*, 170–176.

Jauregui-Renaud, K., Faldon, M. E., Gresty, M. A., & Bronstein, A. M. (2001). Horizontal ocular vergence and the three-dimensional response to whole-body roll motion. *Experimental Brain Research, 136*, 79–92.

Kori, A. A., Schmid-Priscoveanu, A., & Straumann, D. (2002). Otolith effect on torsional quick phases of vestibular nystagmus in humans. *Annals of the New York Academy of Sciences, 956*, 572–573.

Lee, C., Zee, D. S., & Straumann, D. (2000). Saccades from torsional offset positions back to listing's plane. *Journal of Neurophysiology, 83*, 3241–3253.

Mandelli, M. J., Misslisch, H., & Hess, B. J. (2005). Static and dynamic properties of vergence-induced reduction of ocular counter-roll in near vision. *European Journal of Neuroscience, 21*, 549–555.

Migliaccio, A. A., & Todd, M. J. (1999). Real-time rotation vectors. *Australasin Physical & Engineering Sciences in Medicine, 22*, 73–80.

Misslisch, H., Tweed, D., & Hess, B. J. (2001). Stereopsis outweighs gravity in the control of the eyes. *Journal of Neuroscience, 21*, RC126.

Misslisch, H., & Hess, B. J. (2002). Combined influence of vergence and eye position on three-dimensional vestibulo-ocular reflex in the monkey. *Journal of Neurophysiology, 88*, 2368–2376.

Ooi, D., Cornell, E. D., Curthoys, I. S., Burgess, A. M., & MacDougall, H. G. (2004). Convergence reduces ocular counterroll (OCR) during static roll-tilt. *Vision Research, 44*, 2825–2833.

Pansell, T., Schworm, H. D., & Ygge, J. (2003). Torsional and vertical eye movements during head tilt dynamic characteristics. *Investigative Ophthalmology & Visual Science, 44*, 2986–2990.

Peng, G. C., Zee, D. S., & Minor, L. B. (2004). Phase-plane analysis of gaze stabilization to high acceleration head thrusts: a continuum across normal subjects and patients with loss of vestibular function. *Journal of Neurophysiology, 91*, 1763–1781.

Peng, G. C., Minor, L. B., & Zee, D. S. (2005). Gaze position corrective eye movements in normal subjects and in patients with vestibular deficits. *Annals of the New York Academy of Sciences, 1039*, 337–348.

Press, W. H., Flannery, B. P., Teukolsky, S. A., & Vetterling, W. T. (1988). *Numerical recipes in C*. Cambridge, UK: University Press.

Ramat, S., Straumann, D., & Zee, D. S. (2005). The interaural translational VOR: suppression, enhancement and cognitive control. *Journal of Neurophysiology, 94*, 2391–2402.

Ramat, S., & Zee, D. S. (2003). Ocular motor responses to abrupt interaural head translation in normal humans. *Journal of Neurophysiology, 90*, 887–902.

Seidman, S. H., Leigh, R. J., Tomsak, R. L., Grant, M. P., & Dell'Osso, L. F. (1995a). Dynamic properties of the human vestibulo-ocular reflex during head rotations in roll. *Vision Research, 35*, 679–689.

Seidman, S. H., Telford, L., & Paige, G. D. (1995b). Vertical, horizontal, and torsional eye movement responses to head roll in the squirrel monkey. *Experimental Brain Research, 104*, 218–226.

Snyder, L. H., & King, W. M. (1992). Effect of viewing distance and location of the axis of head rotation on the monkey's vestibuloocular reflex. I. Eye movement responses. *Journal of Neurophysiology, 67*, 861–874.

Straumann, D., Zee, D. S., Solomon, D., Lasker, A. G., & Roberts, D. C. (1995). Transient torsion during and after saccades. *Vision Research, 35*, 3321–3334.

Tian, J., Crane, B. T., & Demer, J. L. (2000). Vestibular catch-up saccades in labyrinthine deficiency. *Experimental Brain Research, 131*, 448–457.

Tian, J. R., Crane, B. T., & Demer, J. L. (2003). Vestibular catch-up saccades augmenting the human transient heave linear vestibulo-ocular reflex. *Experimental Brain Research, 151*, 435–445.

Tweed, D., & Vilis, T. (1990). Geometric relations of eye position and velocity vectors during saccades. *Vision Research, 30*, 111–127.

Tweed, D., Sievering, D., Misslisch, H., Fetter, M., Zee, D., & Koenig, E. (1994). Rotational kinematics of the human vestibuloocular reflex. I. Gain matrices. *Journal of Neurophysiology, 72*, 2467–2479.

Tweed, D. (1997). Visual-motor optimization in binocular control. *Vision Research, 37*, 1939–1951.

Viirre, E., Tweed, D., Milner, K., & Vilis, T. (1986). A reexamination of the gain of the vestibuloocular reflex. *Journal of Neurophysiology, 56*, 439–450.